

Comparison of Basicity of the Diimine and Quinoid Group of 1,10-Phenanthroline-5,6-dione Ligated on Pt(II)

Rei Okamura, Tetsuaki Fujihara, Tohru Wada, and Koji Tanaka*

Institute for Molecular Science, 5-1 Higashiyama, Myodaiji, Okazaki 444-8787

CREST, Japan Science and Technology Agency (JST)

Received June 28, 2005; E-mail: ktanaka@ims.ac.jp

A platinum(II) complex bearing 1,10-phenanthroline-5,6-dione ($phenO_2$), $[PtCl(phenO_2\text{-}N,N')(PPh_3)]^+$ ($[\mathbf{2}]^+$) was newly prepared and characterized. An X-ray crystallographic study of $[\mathbf{2}](PF_6)$ revealed that the $phenO_2$ ligand coordinates to platinum with the N,N'-chelate form. The basicity of the quinoid part of $phenO_2$ in $[\mathbf{2}]^+$ and of the diimine one in $[Pt(phenO_2\text{-}O,O')(PPh_3)_2]$ with an O,O'-chelate ring (**3**) was evaluated in the absence and the presence of Li^+ by means of UV–vis spectroscopy and cyclic voltammetry. The quinoid group in $[\mathbf{2}]^+$ practically had no ability to bind Li^+, but induced on anodic potential shift of the $phenO_2$ localized redox potential by 850 mV due to the strong interaction between the reduced form of $[\mathbf{2}]^+$ and Li^+. Undeniably, a weak interaction of Li^+ with the diimine moiety of free $phenO_2$ ($K = 3.6\,M^{-1}$) is greatly enhanced in the interaction between Li^+ and the diimine site in **3** because of the electron donation from the catecholato group of the complex.

Metal complexes bearing electroactive ligands with two or more accessible oxidation states exhibit unique electronic structures resulting from the combination of the oxidation states of the metal and ligands. Dioxolene principally has an ability to coordinate on metals with three different oxidation states; quinone, semiquinonato, and catecholato forms.[1] Metal–dioxolene complexes often feature delocalization of π electrons over the metal and ligands (charge distribution) due to close energy levels between the d orbital of the central metal and π^* orbital of the ligands.[2,3] Polypyridyl–metal complexes also show ligand-localized and metal-centered redox reactions.[4] Intramolecular electron transfer between the two redox sites of metals and ligands often generates characteristic CT bands that are regulated by external stimuli such as photo-irradiation, heat reactions, and redox reactions. Therefore, metal complexes having redox active ligands are feasible candidates for molecular switchings.

The redox behavior of metal–$phenO_2$ complexes ($phenO_2$ = 1,10-phenanthroline-5,6-dione) is of interest because $phenO_2$ has the combined features of polypyridyl and dioxolene ligands. Furthermore, $phenO_2$ has an ability to coordinate to metals with O,O'-chelate (*o*-quinoid form) or N,N'-one (diimine form), or both of them as a bridging ligand connecting two metals.[5–12] Recently, we have reported the redox behavior of Ru(II) complexes having $phenO_2$.[13] We herein report the redox behavior of $Pt^{II}(phenO_2\text{-}N,N')$ having an N,N'-chelate ring and of $Pt^{II}(phenO_2\text{-}O,O')$ with an O,O'-chelate ring to evaluate the basicity of quinoid and diimine groups (Fig. 1).

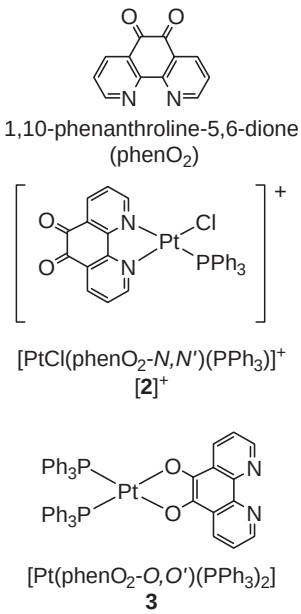

Fig. 1. 1,10-Phenanthroline-5,6-dione ($phenO_2$) and Pt^{II}–$phenO_2$ complexes discussed in this study.

Results and Discussion

Synthesis and Structure of Platinum(II) Complexes. Treatment of $[PtCl_2(PhCN)_2]$ with $phenO_2$ in dimethyl sulfoxide afforded $[PtCl_2(phenO_2\text{-}N,N')]\cdot DMSO$ ($[\mathbf{1}]\cdot DMSO$) as yellow needles (Eq. 1).

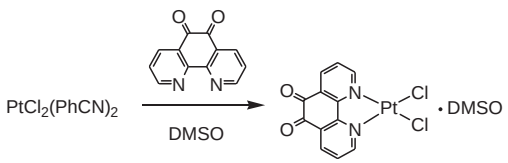

(1)

[1]·DMSO

X-ray crystallography of $[\mathbf{1}]\cdot DMSO$ revealed a square-planar structure of Pt coordinated by two nitrogen atoms of $phenO_2$ and two chlorine atoms.[14] The DMSO molecule of

Published on the web January 13, 2006; DOI 10.1246/bcsj.79.106

[**1**]·DMSO resides as a solvated molecule in a space in the crystal structure. In fact, the ^{1}H NMR spectrum of [**1**]·DMSO in DMSO-d_6 displayed only three signals for phenO_2 protons, indicating a symmetrical structure of the complex. Thus, the molecular structure of [**1**]·DMSO is essentially the same as that of [$PtCl_2$(phenO_2-*N*,*N*′)] (**1**).[15,16] The solubility of [**1**]·DMSO and **1** in organic solvents was too low for measurements of redox behavior of the complexes. Therefore, we introduced PPh_3 into the Pt(phenO_2-*N*,*N*′) framework to improve the solubility of the complex in ordinary solvents. The reaction of **1** with 1 equiv of PPh_3 in CH_3OH at 50 °C for 1.5 h and the subsequent anion exchange gave [PtCl(phenO_2-*N*,*N*′)(PPh_3)](SbF_6) ([**2**](SbF_6)) in moderate yield (Eq. 2).

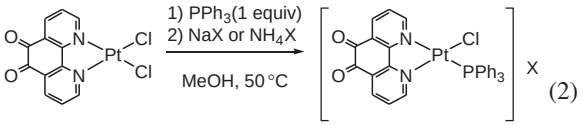

(2)

1 [**2**]$^+$

X = SbF_6, BF_4, PF_6

The ESI-MS spectrum of [**2**]$^+$ in CH_3CN exhibited the parent peak at m/z 703. The IR spectrum of [**2**]$^+$ displayed a strong band at 1709 cm^{-1} assigned to the ν(CO) band. The value is very close to those of **1** (1703 cm^{-1})[15] and [$PtCl_2$(Me$_2$-phenO_2-*N*,*N*′)] (Me$_2$phenO_2 = 2,9-dimethyl-1,10-phenanthroline-5,6-dione) (1699 cm^{-1}),[16] and a slightly higher shifted wavenumber compared with free phenO_2 (1675 cm^{-1}).[5a] The UV–vis spectrum of [**2**](SbF_6) displayed a band at 310 nm, which can be attributed to the intraligand π–π^* transition by analogy with the spectra of [$PtCl_2$(bpy)] (bpy = 2,2′-bipyridine) (313 and 325 nm in DMF) and [Pt(bpy)(PMe_3)$_2$]$^{2+}$ (314 and 324 nm in DMF).[17] On the other hand, [Pt(catecholato)-(PPh_3)$_2$][18] exhibits a characteristic LMCT band in the region of 400 to 500 nm. The appearance of the ν(CO) band at 1709 cm^{-1} in the IR spectrum and the absence of absorption bands in the region of 400 to 500 nm in the electronic absorption spectrum of [**2**]$^+$ indicate that phenO_2 is bound to Pt with the *N*,*N*′-chelate.

Figure 2 shows the ORTEP view of [**2**]$^+$ determined by X-ray crystallography. The details of data collection, refinement for the complex, and selected bond lengths and angles are listed in Table 1 and 2, respectively. The Pt atom is coordinated in square-planar form with two nitrogen, one chlorine, and one phosphorus atom. Molecular structures of Pt(II) complexes are subject to the steric hindrance of ligands. For example, two

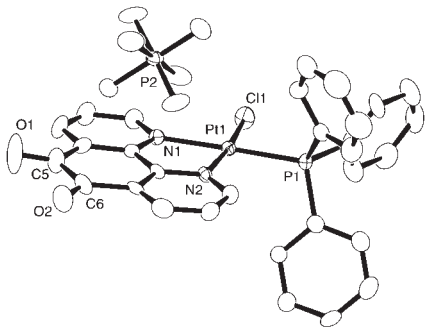

Fig. 2. ORTEP drawing of [**2**](PF_6) with 50% thermal ellipsoids. Hydrogen atoms are omitted for clarity.

Table 1. Crystallographic Data for Complex [**2**](PF_6)

	[**2**](PF_6)
Formula	$C_{30}H_{21}ClF_6N_2O_2P_2Pt$
Formula weight	847.99
Color	Pale_Yellow
Crystal size/mm^3	0.40 × 0.10 × 0.05
Crystal system	orthorhombic
Space group	*Pbca*
a/Å	14.391(5)
b/Å	14.998(6)
c/Å	27.80(1)
α/deg	90
β/deg	90
γ/deg	90
V/Å^3	6000(1)
Z	8
T/K	−173
D_{calcd}/g cm^{-3}	1.877
Radiation	Mo Kα (λ = 0.71070 Å)
μ/cm^{-1}	49.24
F(000)	3280.00
$2\theta_{max}$/deg	55.0
No. of reflections (all, $2\theta < 54.97°$)	6787
No. of variables	397
Reflection/Parameter Ratio	17.10
GOF	1.27
$R1$[a] [$I > 2\sigma(I)$]	0.056
R[b] (all data)	0.082
R_w[c] (all data)	0.139

a) $R1 = \Sigma||F_o| - |F_c||/\Sigma|F_o|$. b) $R = \Sigma(F_o^2 - F_c^2)/\Sigma F_o^2$. c) $R_w = [(\Sigma\omega(F_o^2 - F_c^2)^2/\Sigma\omega(F_o^2)^2)]^{1/2}$.

Table 2. Selected Bond Lengths and Bond Angles of [**2**](PF_6)

Bond	Lengths/Å	Bond	Lengths/Å
Pt1–Cl1	2.270(2)	C5–O1	1.20(1)
Pt1–P1	2.255(2)	C6–O2	1.19(1)
Pt1–N1	2.079(6)	C5–C6	1.54(1)
Pt1–N2	2.043(6)		
Bond	**Angles/deg**	**Bond**	**Angles/deg**
Cl1–Pt1–P1	91.18(8)	P1–Pt1–N2	96.2(2)
Cl1–Pt1–N1	92.6(2)	N1–Pt1–N2	80.0(2)

chlorine and two nitrogen atoms coordinated on [$PtCl_2$(Me$_2$-phenO_2-*N*,*N*′)] largely deviate out of plane due to the steric repulsion induced by two Me-groups.[16] In addition, Me$_2$phen of [PtI_2(Me$_2$phen)(PPh_3)] (Me$_2$phen = 2,9-dimethyl-1,10-phenanthlorine) is linked to Pt in a monodentate manner.[19] The square-planar structure of [**2**]$^+$ exhibits less steric repulsion between phenO_2 bonded to Pt with the diimine group and bulky PPh_3. The Pt–N distances (Pt1–N1, 2.079(6) Å and Pt1–N2, 2.043(6) Å) are close to those of previously reported crystal structures having a Pt–bipyridyl skeleton.[20] The Pt–Cl bonding (Pt1–Cl1, 2.270(2) Å) is also in good agreement with those of [PtCl(bpy)(L)] and [PtCl(phen)(L)] (L = extra ligand)

complexes.[21] The Pt–P distance (Pt1–P1, 2.255(2) Å) is comparable to that of $[PtMe(Me_2phen)(PPh_3)]^+$.[22] The two C=O double bond distances are 1.20(1) and 1.19(1) Å, which are in good agreement with that of metal–free phenO$_2$ (1.209(3) Å)[9a] and those of other metal–phenO$_2$ complexes.[13,23] Platinum(II)–polypyridyl complexes tend to form $\pi\cdots\pi$ or Pt···Pt stacking columns in the crystal structure.[24] On the other hand, the Pt···Pt atomic distance of 7.55 Å in the crystal structure of $[\mathbf{2}]^+$ is an implication of no interaction between the neighboring two Pt metals. In addition, PF_6^- is positioned between two phenO$_2$ ligands of the adjacent molecules. The bulky PPh_3 of $[\mathbf{2}]^+$ may be responsible for blocking the formation of intermolecular Pt···Pt and $\pi\cdots\pi$ stackings in the solid state.

Electronic Spectra of Pt(II) Complexes in the Presence of Lewis Acids. The complex $[\mathbf{2}]^+$ has an *N*,*N*′-chelate ring with a free quinoid group. We obtained [Pt(phenO$_2$-*O*,*O*′)(PPh$_3$)$_2$] (**3**), which has an *O*,*O*′-chelate ring with a free diimine site, by the reaction of [Pt(PPh$_3$)$_4$] with phenO$_2$ in CH_2Cl_2.[25] The difference in the coordination modes of phenO$_2$ in $[\mathbf{2}]^+$ and **3** results from the strong π acceptor character of a quinoid group and strong σ donor ability of a diimine group. The complex $[\mathbf{2}]^+$ bearing the Pt^{II}(phenO$_2$-*N*,*N*′) framework is formed by a nucleophilic attack of the diimine of phenO$_2$ on Pt(II). On the other hand, the formation of **3** with the Pt^{II}(phenO$_2$-*O*,*O*′) framework is ascribed to an electrophilic attack of the quinone of phenO$_2$ to Pt(0) and the subsequent intramolecular electron transfer from the low valent metal center to the ligand. The basicity of the quinoid moieties of phenO$_2$ in $[\mathbf{2}]^+$ would be substantially decreased compared with that of free phenO$_2$, whereas the electron densities of the diimine group of phenO$_2$ in **3** would be greatly increased compared with that of free phenO$_2$. The basicity of the diimine and quinoid groups of $[\mathbf{2}]^+$ and **3** were estimated by the electronic absorption spectra in the presence of Lewis acids.

An addition of 1.0 equiv of aqueous $HClO_4$ solution to a CH_3CN solution of [**2**](SbF$_6$) did not cause any changes in the electronic absorption spectrum or ESI-MS spectrum of the complex. Therefore, the interaction between $[\mathbf{2}]^+$ and $HClO_4$ is extremely low or practically not detected under the experimental conditions. On the other hand, an addition of $HClO_4$ to a CH_3CN solution of **3** resulted in degradation of the complex, because the parent peak of the ESI-MS spectrum of **3** (m/z 930 ($[\mathbf{3}]^+$)) decreased in intensity with increasing amounts of $HClO_4$ added and a new peak of m/z 796 corresponding to $[PtCl(CH_3CN)(PPh_3)_2]^+$ appeared, even in the presence of 0.1 equiv of $HClO_4$ in CH_3CN. Taking into account that the phenO$_2$ of **3** is linked to Pt(II) with the catecholato form, dissociation of phenO$_2$ from Pt(II) in the presence of $HClO_4$ is explained by the protonation of the catecholato oxygens. Thus, $HClO_4$ is too strong a Lewis acid to evaluate the basicity of the diimine group of **3**. Therefore, we examined the interaction of $[\mathbf{2}]^+$ and **3** with $LiBF_4$ in place of $HClO_4$ in CH_3CN. As in the case of the interaction between $[\mathbf{2}]^+$ with H^+, the absorption spectra of [**2**](SbF$_6$) in the presence of a large excess of $LiBF_4$ in CH_3CN did not give any evidence of an interaction between $[\mathbf{2}]^+$ and Li^+ in the solution. On the other hand, an addition of $LiBF_4$ to a CH_3CN solution of **3** resulted in a decrease in the absorption band at 373 nm, and an appearance of two new bands at 328 and 396 nm. The spectral changes almost stopped after one equiv of Li^+ was added to the solution, during which four isosbestic points appeared at 350, 394, 436, and 480 nm (Fig. 3). Further addition of Li^+ to the solution did not cause any changes in the spectrum. Thus, Li^+ and **3** almost quantitatively formed a 1:1 adduct in CH_3CN (Eq. 3).[26] An addition of $HClO_4$ to **3** caused degradation of

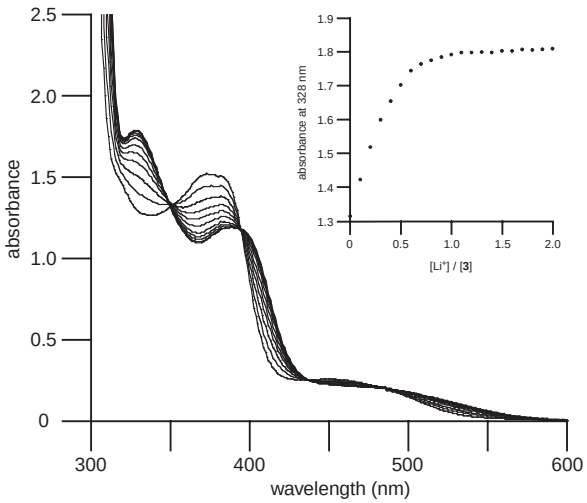

Fig. 3. The electronic absorption spectra of **3** (0.200 mM) in the presence of various amounts of $LiBF_4$ (0–1.0 equiv) in CH_3CN. Inset: titration of **3** with $LiBF_4$ in CH_3CN at 328 nm.

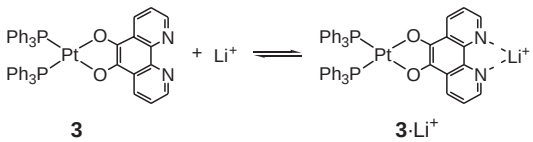

3 **3**·Li$^+$ (3)

the complex, probably due to protonation of the catecholato oxygens. On the other hand, the most reasonable binding site of Li^+, is the diimine nitrogen of **3**, since only a 1:1 adduct is formed between Li^+ and **3**, even in the presence of a large excess of Li^+ in solution. Indeed, the ESI-MS spectrum of **3** in the presence of 10 equiv of Li^+ showed a peak of m/z 937 assignable to **3**·Li^+ besides a parent peak (m/z 930 ($[\mathbf{3}]^+$)). The phenO$_2$ ligand bonded to Pt(II) with the two-electron reduced form (see below) endowed such a strong basicity to the diimine group to bind Li^+ almost quantitatively.

We also examined the interaction between free phenO$_2$ and Li^+ to evaluate the degree of the increase in basicity of the phenO$_2$ of **3** compared with that of the free ligand. The electronic absorption spectrum of phenO$_2$ shows two absorption bands at 296 and 308 nm in CH_3CN (Fig. 4). An addition of $LiBF_4$ to the solution results in an increase in the intensity of those bands. The two bands continuously increase in intensity with increasing amounts of Li^+ added to the solution and merges at 308 nm in the presence of more than 100 equiv of Li^+. The appearance of an isosbestic point at 279 nm that remained unchanged irrespective of the amounts of $LiBF_4$ is indication of the 1:1 adduct formation between phenO$_2$ and Li^+ in CH_3CN (Eq. 4). The binding constant K for the adduct formation between phenO$_2$ and Li^+ was calculated according to Eqs. 4–6. In the above equation, A_0 and A are the absorbance of phenO$_2$ at 296 nm in the absence and in the presence

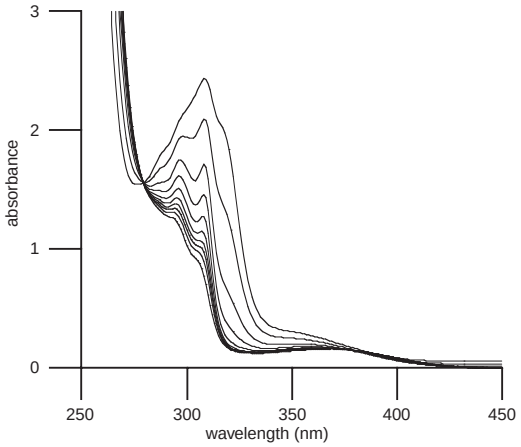

Fig. 4. The electronic absorption spectra of $phenO_2$ (0.305 mM) in the presence of various amounts of $LiBF_4$ (0–200 equiv) in CH_3CN.

$$phenO_2 + Li^+ \rightleftharpoons phenO_2 \cdot Li^+, \quad (4)$$

$$K = \frac{c_{phenO_2Li}}{c_{phenO_2} \cdot c_{Li}}, \quad (5)$$

$$\frac{1}{(A_0 - A)} = \frac{1}{K \cdot X} \cdot \frac{1}{c_{Li}} + \frac{1}{X}, \quad (6)$$

where $X = c_{phenO_2} \cdot \varepsilon_{phenO_2} + c_{phenO_2Li} \cdot \varepsilon_{phenO_2Li}$

of Li^+, respectively, c_{phenO_2}, c_{Li}, and c_{phenO_2Li} are the concentrations of $phenO_2$, Li^+, and complexed $phenO_2 \cdot Li^+$, respectively, and ε_{phenO_2} and ε_{phenO_2Li} are the molar extinction coefficients of $phenO_2$ and complexed $phenO_2 \cdot Li^+$, respectively. A plot of $1/(A_0 - A)$ against $1/c_{Li}$ gave a straight line in the presence of more than 20 equiv of Li^+. The binding constant K obtained from the intercept was $3.6\,M^{-1}$. The binding constant for the adduct formation with Li^+ therefore increases in the order of $[\mathbf{2}]^+ \ll phenO_2 \ll \mathbf{3}$. The trend is apparently proportional to the electron density of the diimine moiety depending on the amount of electrons transfered from the *o*-quinoid part of $phenO_2$.

Redox Behavior of $[2]^+$ and 3 in the Absence and the Presence of Li^+. The cyclic voltammogram (CV) of $[\mathbf{2}](SbF_6)$ in CH_3CN displayed two reversible redox couples at $E^1{}_{1/2} = -0.02\,V$ and $E^2{}_{1/2} = -0.75\,V$ (vs SCE), and an irreversible cathodic wave at $E^3{}_{pc} = -1.80\,V$ (Fig. 5a). The equilibrium electrode potential (E_{rest}) of the solution (+0.32 V) also supported the quinoid form of $phenO_2$ in $[\mathbf{2}]^+$. The reversible redox reactions at $E^1{}_{1/2}$ and $E^2{}_{1/2}$ are assigned to the ligand-based quinone/semiquinonato and semiquinonato/catecholato couples, respectively, and the irreversible one at $E^3{}_{pc}$ is associated with the reduction of the central metal. Based on the redox potential of free $phenO_2$ ($E^1{}_{1/2} = -0.45\,V$ and $E^2{}_{1/2} = -1.25$ V),[5a] coordination of $phenO_2$ on Pt(II) resulted in an anodic shift of the redox potential of the ligand by about 400–500 mV due to the electron donation from $phenO_2$ to Pt(II) through the diimine chelate. As discussed above, the electronic absorption spectra of $[\mathbf{2}]^+$ did not display any interactions with Li^+ in CH_3CN.[27] On the other hand, an addition of 1 equiv of $LiBF_4$ to the CH_3CN solution of $[\mathbf{2}]^+$ caused an anodic shift of the redox couple at $E^1{}_{1/2} = -0.02\,V$ and $E^2{}_{1/2} = -0.75\,V$ by 850 and 120 mV, respectively (Fig. 5b), and the two redox couples

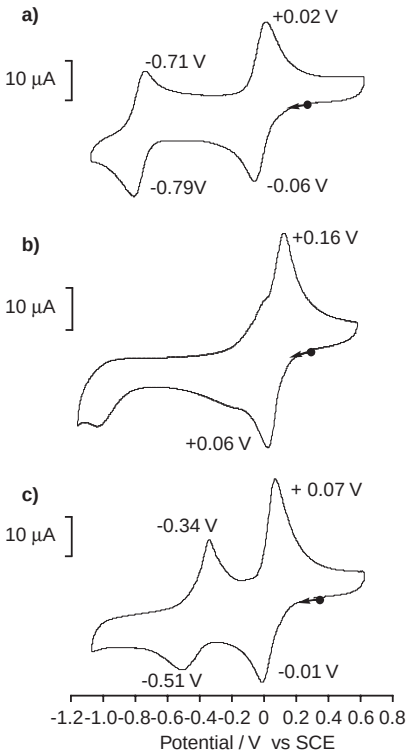

Fig. 5. Cyclic voltammograms of $[\mathbf{2}]^+$ (1.0 mM) in the absence (a) and the presence of 1.0 equiv of $LiBF_4$ (b) and $NaClO_4$ (c) in CH_3CN containing 0.1 M $^nBu_4NPF_6$. The dot in the voltammograms is the equilibrium electrode potential of the solutions.

fused into one peak at $E_{pa} = +0.16\,V$ and $E_{pc} = +0.06\,V$. Further addition of Li^+ hardly had any influences on the pattern of the CV, indicating that the $phenO_2$ of $[\mathbf{2}]^+$ has no ability to bind Li^+. However, Li^+ greatly facilitates the two-electron reduction of $[\mathbf{2}]^+$ through an ECE mechanism. As a result, the resultant $[\mathbf{2}]^-$ quantitatively binds Li^+ with the *O*,*O*′-chelate. As in the case of $LiBF_4$, $NaClO_4$ also caused anodic shifts of the redox potentials of $[\mathbf{2}]^+$, since two redox waves appeared at $E_{pc} = -0.01\,V$ and at $E_{pc} = -0.51\,V$ in the presence of 1 equiv of $NaClO_4$ in CH_3CN. However, the appearance of a spike anodic wave at $E_{pa} = +0.07\,V$ in the reverse potential scans is an implication of adsorption of the adduct between $[\mathbf{2}]$ and Na^+ on the surface of the glassy carbon working electrode due to low solubility of the adduct (Fig. 5c).

The CV of **3** in CH_3CN displayed the reversible catecholato/semiquinonato redox couple and an irreversible semiquinonato/quinone one at $E^1{}_{1/2} = +0.28\,V$ and $E^2{}_{pa} = +0.81\,V$, respectively.[6] The appearance of the equilibrium electrode potential of the solution ($E_{rest} = +0.03\,V$) at the negative site of the $E^1{}_{1/2}$ and $E^2{}_{pa}$ redox reactions indicates that $phenO_2$ is linked to Pt with the catecholato form, not the semiquinonato one. The irreversible semiquinonato/quinone redox couple in the CV of **3** is ascribed to lability of the quinoid structure of **3** due to the extremely weak electron donor ability of the quinoid group.[6] In contrast to $[\mathbf{2}]^+$, **3** appears to bind Li^+ in CH_3CN quantitatively. The redox wave at $E^1{}_{1/2} = +0.28\,V$ gradually shifted to positive potentials with increasing the concentration of Li^+ (Fig. 6). The shift of the redox waves almost stopped in

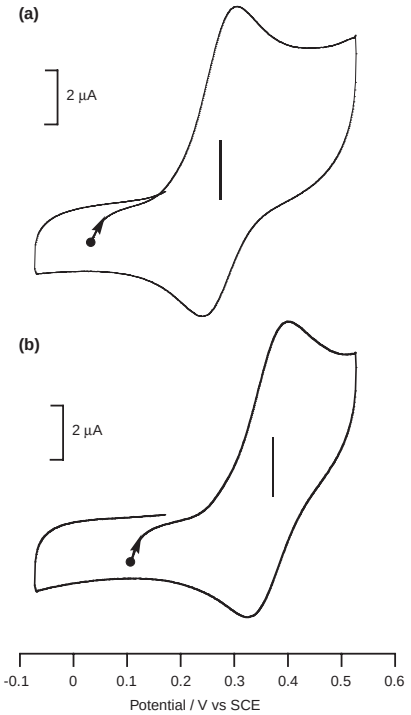

Fig. 6. Cyclic voltammograms of **3** (0.50 mM) in the absence (a) and the presence of 1.0 equiv of $LiBF_4$ (b) in CH_3CN containing 0.1 M $^nBu_4NPF_6$. The dot in the voltammograms is the equilibrium electrode potential of the solutions.

the presence of 1.0 equiv of $LiBF_4$, where the catecholato/semiquinonato redox couple of **3** is observed at $E^{1\prime}{}_{1/2} = +0.37$ V. The fact that **3** forms only the 1:1 adduct with Li^+ indicates that Li^+ does not attack the catecholato oxygens of **3**. It is worthy to note that the difference in the redox potentials of the catecholato/semiquinonato couple of $[\mathbf{2}]^+$ and **3** in the absence and in the presence of Li^+ are $\Delta E^1{}_{1/2} = 850$ mV and $\Delta E^1{}_{1/2} = 90$ mV, respectively. The change in the electron density of the quinoid moiety in $[\mathbf{2}]^+$ and **3** caused by the redox reactions at $E^1{}_{1/2}$ and $E^2{}_{1/2}$ is apparently much larger than that of the diimine one, because the phenanthroline moiety of phenO$_2$ plays a central role in the ligand-based redox reactions. As a result, the basicity of the quinoid oxygens exhibits great changes upon the phenO$_2$ localized redox reaction, whereas the redox reactions have minor effects on the change of the electron density of the diimine group.

Experimental

Materials. Commercially available $[K_2PtCl_4]$ and triphenylphosphine were used without further purification. The tetrabutylammonium hexafluorophosphate used as a supporting electrolyte for electrochemistry was recrystallized from hot ethanol. 1,10-Phenanthroline-5,6-dione (phenO$_2$),[28] $[PtCl_2(PhCN)_2]$,[29] $[PtCl_2$-(phenO$_2$-*N*,*N*′)] (**1**),[15] and [Pt(phenO$_2$-*O*,*O*′)(PPh$_3$)$_2$] (**3**)[25] were prepared according to the literature.

Preparations of Complexes. [PtCl$_2$(phenO$_2$-*N*,*N*′)]·DMSO, [1]·DMSO: To a dimethyl sulfoxide solution (4 mL) of $[PtCl_2$-$(PhCN)_2]$ (54.5 mg, 0.115 mmol) was added a dimethyl sulfoxide solution (2 mL) of 1,10-phenanthroline-5,6-dione (24.2 mg, 0.115 mmol). On standing overnight at room temperature, yellow crystals formed out of the reaction mixture. The crystals were collected by filtration, washed with diethyl ether and dried in vacuo. Yield: 47.1 mg (0.085 mmol, 74%). Anal. Found: C, 30.07; H, 2.20; N, 4.99%. Calcd for $C_{14}H_{12}Cl_2N_2O_3PtS$: C, 30.33; H, 2.18; N, 5.05%. ^{1}H NMR (500 MHz, DMSO-d_6, rt, δ/ppm): 8.07 (dd, J(H–H) = 6.0, 8.0 Hz, 2H, phenO$_2$), 8.84 (dd, J(H–H) = 1.0, 8.0 Hz, 2H, phenO$_2$), 9.59 (dd, J(H–H) = 1.0, 6.0 Hz, 2H, phenO$_2$).

[(PtCl)(phenO$_2$-*N*,*N*′)(PPh$_3$)](SbF$_6$), [2](SbF$_6$): A methanol suspension (80 mL) of $[PtCl_2$(phenO$_2$-*N*,*N*′)] (82.3 mg, 0.173 mmol) and triphenylphosphine (45.3 mg, 0.173 mmol) was warmed to 50 °C for 1.5 h under N_2. The resulting yellow solution was filtered to remove unreacted $[PtCl_2$(phenO$_2$-*N*,*N*′)]. The addition of a saturated aqueous solution of $NaSbF_6$ to the filtrate precipitated yellow solids, which were separated by filtration, washed with water and then diethyl ether, and dried in vacuo. Yield: 111.1 mg (0.118 mmol, 68%). Anal. Found: C, 37.78; H, 2.37; N, 2.94%. Calcd for $C_{30}H_{21}ClF_6N_2O_2PPtSb\cdot(H_2O)$: C, 37.66; H, 2.42; N, 2.93%. ^{1}H NMR (500 MHz, CD_3CN, rt, δ/ppm): 7.29 (m, 1H, phenO$_2$), 7.54 (m, 6H, PPh$_3$), 7.66 (m, 3H, PPh$_3$), 7.89 (m, 6H, PPh$_3$), 8.06 (m, 1H, phenO$_2$), 8.15 (m, 1H, phenO$_2$), 8.67 (d, J(H–H) = 8.0 Hz, 1H, phenO$_2$), 8.88 (d, J(H–H) = 8.0 Hz, 1H, phenO$_2$), 9.74 (m, 1H, phenO$_2$). IR (ν/cm^{-1}, KBr): 1709 (CO). ESI-MS (m/z, CH_3CN): 703 ($[\mathbf{2}]^+$). UV–vis (λ_{max}/nm (ε/M^{-1} cm^{-1}), CH_3CN): 310 (9100).

[(PtCl)(phenO$_2$-*N*,*N*′)(PPh$_3$)](BF$_4$), [2](BF$_4$): The complex was prepared by a similar method to that of [**2**](SbF_6) using $NaBF_4$ instead of $NaSbF_6$. Yield: 64%. Anal. Found: C, 45.11; H, 2.86; N, 3.48%. Calcd for $C_{30}H_{21}BClF_4N_2O_2PPt\cdot0.5(H_2O)$: C, 45.11; H, 2.78; N, 3.51%.

[(PtCl)(phenO$_2$-*N*,*N*′)(PPh$_3$)](PF$_6$), [2](PF$_6$): The complex was prepared by a similar method to that of [**2**](SbF_6) using NH_4PF_6 instead of $NaSbF_6$. Yield: 81%. Anal. Found: C, 42.33; H, 2.62; N, 3.46%. Calcd for $C_{30}H_{21}ClF_6N_2O_2P_2Pt$: C, 42.49; H, 2.50; N, 3.50%.

Measurements. ^{1}H NMR was performed with a JEOL GX-500 spectrometer. Infrared spectra were recorded on a Shimadzu FT IR-8100 spectrophotometer. ESI-MS spectra were measured with a Shimadzu LCMS-2010 liquid chromatograph mass spectrometer and a Waters Micromass LCT. Elemental analyses were carried out at the Research Center for Molecular-Scale Nanoscience, Institute for Molecular Science. Cyclic voltammetry was performed with an ALS/Chi model 660 electrochemical analyzer. Cyclic voltammograms were recorded at a scan rate of 100 mV s^{-1} at room temperature using a glassy carbon working electrode, a Pt wire counter electrode and a $Ag/AgNO_3$ (0.01 mmol dm^{-3}) reference electrode. All potentials were converted to SCE ($E_{SCE} = E_{Ag/Ag^+} + 0.327$ V). UV–vis spectra were recorded on a Shimadzu UV-3100PC UV–vis–NIR scanning spectrophotometer and a Hewlett-Packard 8453 diode array spectrophotometer.

Crystallography. Pale yellow crystals of [**2**](PF_6) were obtained by vapor diffusion of diethyl ether into an acetonitrile solution of the complex. The crystal data of [**2**](PF_6) are summarized in Table 1. Data for [**2**](PF_6) were collected on a Rigaku/MSC Mercury CCD diffractometer using graphite-monochromated Mo Kα radiation ($\lambda = 0.71070$ Å) at 173 K, and processed using CrystalClear.[30] A numerical absorption correction was carried out and the data were corrected for Lorentz and polarization effects. The structure was solved by direct methods (SIR92)[31] and refined by full-matrix least-squares refinement on F^2. All non-hydrogen atoms were refined anisotropically. All hydrogen atoms were located in the calculated positions and not refined. All calculations were performed using the teXsan crystallographic software

package.[32] Crystallographic data have been deposited with Cambridge Crystallographic Data Centre: Deposition number CCDC-280916 for compound [**2**](PF_6). Copies of the data can be obtained free of charge via http://www.ccdc.cam.ac.uk/conts/retrieving.html (or from the Cambridge Crystallographic Data Centre, 12, Union Road, Cambridge, CB2 1EZ, UK; Fax: +44 1223 336033; e-mail: deposit@ccdc.cam.ac.uk).

Supporting Information

Tables of crystallographic data (Table S1), selected bond distances and angles (Table S2), and the ORTEP drawing (Fig. S1) for [**1**]·DMSO are formatted in PDF files. This material is available free of charge on the web at: http://www.csj.jp/journals/bcsj/.

References

1 a) C. G. Pierpont, R. M. Buchanan, *Coord. Chem. Rev.* **1981**, *38*, 45. b) C. G. Pierpont, C. W. Lange, *Prog. Inorg. Chem.* **1994**, *41*, 331. c) C. G. Pierpont, *Coord. Chem. Rev.* **2001**, *216–217*, 99. d) M. D. Ward, J. A. McCleverty, *J. Chem. Soc., Dalton Trans.* **2002**, 275.

2 a) M. Haga, E. S. Dodsworth, A. B. P. Lever, S. R. Boone, C. G. Pierpont, *J. Am. Chem. Soc.* **1986**, *108*, 7413. b) S. R. Boone, C. G. Pierpont, *Inorg. Chem.* **1987**, *26*, 1769. c) S. Bhattacharya, S. R. Boone, G. A. Fox, C. G. Pierpont, *J. Am. Chem. Soc.* **1990**, *112*, 1088. d) S. Bhattacharya, C. G. Pierpont, *Inorg. Chem.* **1991**, *30*, 1511. e) S. Bhattacharya, C. G. Pierpont, *Inorg. Chem.* **1994**, *33*, 6038.

3 a) M. Haga, E. S. Dodsworth, A. B. P. Lever, *Inorg. Chem.* **1986**, *25*, 447. b) A. B. P. Lever, P. R. Auburn, E. S. Dodsworth, M. Haga, W. Liu, M. Melnik, W. A. Nevin, *J. Am. Chem. Soc.* **1988**, *110*, 8076. c) H. Masui, A. B. P. Lever, P. R. Auburn, *Inorg. Chem.* **1991**, *30*, 2402. d) P. R. Auburn, E. S. Dodsworth, M. Haga, W. Liu, W. A. Nevin, A. B. P. Lever, *Inorg. Chem.* **1991**, *30*, 3502.

4 a) J. P. Sauvage, J. P. Collin, J. P. Chambron, S. Guillerez, C. Coudret, V. Balzani, F. Barigelletti, L. De Cola, L. Flamingi, *Chem. Rev.* **1994**, *94*, 993. b) V. Balzani, A. Juris, M. Venturi, S. Campagna, S. Serroni, *Chem. Rev.* **1996**, *96*, 759.

5 a) C. A. Goss, H. D. Abruña, *Inorg. Chem.* **1985**, *24*, 4263. b) Q. Wu, M. Maskus, F. Pariente, F. Tobalina, V. M. Fernandez, E. Lorenzo, H. D. Abruña, *Anal. Chem.* **1996**, *68*, 3688.

6 G. A. Fox, S. Bhattacharya, G. C. Pierpont, *Inorg. Chem.* **1991**, *30*, 2895.

7 a) W. Paw, R. Eisenberg, *Inorg. Chem.* **1997**, *36*, 2287. b) W. Paw, W. B. Connick, R. Eisenberg, *Inorg. Chem.* **1998**, *37*, 3919.

8 P. L. Hill, L. Y. Lee, L. T. R. Younkin, S. D. Orth, L. McElwee-White, *Inorg. Chem.* **1997**, *36*, 5655.

9 a) F. Calderazzo, F. Marchetti, G. Pampaloni, V. Passarelli, *J. Chem. Soc., Dalton Trans.* **1999**, 4389. b) F. Calderazzo, G. Pampaloni, V. Passarelli, *Inorg. Chim. Acta* **2002**, *330*, 136.

10 A. D. Shukla, A. Das, *Polyhedron* **2000**, *19*, 2605.

11 Y. Lei, C. Shi, F. C. Anson, *Inorg. Chem.* **1996**, *35*, 3044.

12 G. Hilt, T. Jarbawi, W. R. Heineman, E. Steckhan, *Chem. Eur. J.* **1997**, *3*, 79.

13 a) T. Fujihara, R. Okamura, T. Wada, K. Tanaka, *Dalton Trans.* **2003**, 3221. b) T. Fujihara, T. Wada, K. Tanaka, *Dalton Trans.* **2004**, 645.

14 In the result of X-ray crystallography of [**1**]·DMSO, all atoms except for platinum atom were not refined anisotropically. However, the structure revealed that $phenO_2$ ligand coordinates on diimine site and that platinum atom shows square-planar coordination. See Supporting Information.

15 R. C. Conrad, J. V. Rund, *Inorg. Chem.* **1972**, *11*, 129.

16 N. Margiotta, V. Bertolasi, F. Capitelli, L. Maresca, A. G. G. Moliterni, F. Vizza, G. Natile, *Inorg. Chim. Acta* **2004**, *357*, 149.

17 a) S. S. Kamath, V. Uma, T. S. Srivastava, *Inorg. Chim. Acta* **1989**, *161*, 49. b) D. Collison, F. E. Mabbs, E. J. L. McInnes, K. J. Taylor, A. J. Welch, L. J. Yellowllees, *J. Chem. Soc., Dalton Trans.* **1996**, 329.

18 a) S. Cenini, R. Ugo, G. La Monica, *J. Chem. Soc. A* **1971**, 416. b) N. M. Shavaleev, L. P. Moorcraft, S. J. A. Pope, Z. R. Bell, S. Faulkner, M. D. Ward, *Chem. Eur. J.* **2003**, *9*, 5283.

19 a) F. P. Fanizzi, L. Maresca, G. Natile, M. Lanfranchi, A. Tiripicchio, G. Pacchioni, *J. Chem. Soc., Chem. Commun.* **1992**, 333. b) F. P. Fanizzi, M. Lanfranchi, G. Natile, A. Tiripicchio, *Inorg. Chem.* **1994**, *33*, 3331.

20 a) A. Hazell, A. Mukhopadhyay, *Acta Crystallogr., Sect. B* **1980**, *36*, 1647. b) H.-Q. Liu, S.-M. Peng, C. M. Che, *Chem. Commun.* **1995**, 509. c) M. Hissler, W. B. Connick, D. K. Geiger, J. E. McGarrah, D. Lipa, R. J. Lachicotte, R. Eisenberg, *Inorg. Chem.* **2000**, *39*, 447. d) M. E. Cucciolito, V. De Felice, F. Giordano, I. Orabona, F. Ruffo, *Eur. J. Inorg. Chem.* **2001**, 3095.

21 a) R. H. Herber, M. Croft, M. J. Coyer, B. Bilash, A. Sahiner, *Inorg. Chem.* **1994**, *33*, 2422. b) A. Doppiu, M. A. Cinellu, G. Minghetti, S. Stoccoro, A. Zucca, M. Manassero, M. Sansoni, *Eur. J. Inorg. Chem.* **2000**, 2555.

22 R. Romeo, L. Fenech, L. M. Scolaro, A. Albinati, A. Macchioni, C. Zuccaccia, *Inorg. Chem.* **2001**, *40*, 3293.

23 a) T. M. Santos, B. J. Goodfellow, J. Madureira, J. Pedrosa de Jesus, V. Félix, M. G. B. Drew, *New J. Chem.* **1999**, *23*, 1015. b) R. Ruiz, A. Caneschi, D. Gatteschi, A. B. Gaspar, J. A. Real, I. Fernandez, M. C. Muñoz, *Inorg. Chem. Commun.* **1999**, *2*, 521.

24 a) H.-K. Yip, L.-K. Cheng, K.-K. Cheung, C.-M. Che, *J. Chem. Soc., Dalton Trans.* **1993**, 2933. b) J. A. Bailey, M. G. Hill, R. E. Marsh, V. M. Miskowski, W. P. Schaefer, H. B. Gray, *Inorg. Chem.* **1995**, *34*, 4591. c) R. Palmans, D. B. MacQueen, C. G. Pierpont, A. J. Frank, *J. Am. Chem. Soc.* **1996**, *118*, 12647. d) R. Büchner, C. T. Cummingham, J. S. Field, R. J. Haines, D. R. McMillin, G. C. Summerton, *J. Chem. Soc., Dalton Trans.* **1999**, 711. e) S.-W. Lai, M. C. W. Chan, K.-K. Cheung, C.-M. Che, *Inorg. Chem.*, **1999**, *38*, 4262. f) R. Romeo, L. M. Scolaro, M. R. Plutino, A. Albinati, *J. Organomet. Chem.* **2000**, *593–594*, 403. g) V. W.-W. Yam, R. P.-L. Tang, K. M.-C. Wong, K.-K. Cheung, *Organometallics* **2001**, *20*, 4476.

25 A. Y. Girgis, Y. S. Sohn, A. Balch, *Inorg. Chem.* **1975**, *14*, 2327.

26 The ESI-MS spectrum demonstrated that **3** forms not only the **3**:Li^+ (1:1 adduct: m/z 930) but also the 2:1 one (m/z 1867) with Li^+ when the concentration of the former is much higher than the latter (**3** $\gg$ Li^+). However, the amount of the 2:1 adduct became negligible small in the presence of more than 0.9 equiv of Li^+. The binding constant for the 1:1 adduct (Eq. 4) was evaluated as $K = 3 \times 10^6\,M^{-1}$ from the spectrum changes of Fig. 3 under such the conditions.

27 In the solution IR spectra, the ν(CO) band of [**2**]$^+$ at $1709\,cm^{-1}$ in CD_3CN remained unchanged irrespective of the absence and presence of 2 equiv of $LiBF_4$. Because of an intense absorption of BF_4^-, we could not see the area in $1580–1680\,cm^{-1}$.

28 M. Yamada, Y. Tanaka, Y. Yoshimoto, S. Kuroda, I. Shimao, *Bull. Chem. Soc. Jpn.* **1992**, *65*, 1006.

29 P. Braunstein, R. Bender, J. Jud, *Inorg. Synth.* **1987**, *26*,

341.
30 *CrystalClear: Software Package*, Rigaku and Molecular Structure Corporation, **1999**.
31 *SIR92*, A. Altomare, G. Cascarano, C. Giacovazzo, A. Guagliardi, *J. Appl. Crystallogr.* **1993**, *26*, 343.
32 *teXsan: Crystal Structure Analysis Package*, Molecular Structure Corporation, **1985** and **1999**.